OPTIMAL IMPULSIVE COLLISION AVOIDANCE

Claudio Bombardelli*

The problem of optimal impulsive collision avoidance between two colliding objects in 3-dimensional elliptical Keplerian orbits is investigated with the purpose of establishing the optimal impulse direction and orbit location that give rise to the maximum miss distance following the maneuver. Closed-form analytical expressions are provided that predicts such distance and can be employed to perform a full optimization analysis. After verifying the accuracy of the expression for any orbital eccentricity and encounter geometry the optimum maneuver direction is derived as a function of the arc length separation between the maneuver point and the predicted collision point. The provided formulas can be used for high-accuracy instantaneous estimation of the outcome of a generic impulsive collision avoidance maneuver and its optimization.

INTRODUCTION

The accumulation of space debris in low and geostationary Earth orbit is threatening the future of space utilization and calls for immediate action. One way to limit the continuous growth of the space objects' population is to prevent collisions involving massive satellites and rocket bodies. Along this line, three types of mitigation measures have been considered: post-mission disposal (PMD) of satellites and upper stages, active collision avoidance (ACA) of maneuverable satellites and active debris removal (ADR) of defunct satellites and upper stages left in orbit. While no ADR operation has yet taken place (due to its high technological complexity) PMD and ACA are conducted routinely.

Typically, an ACA evasive maneuver is performed following a conjunction event whose collision probability exceeds a limit threshold of 10^{-4}. Depending on the accuracy of the tracking system the "reaction time" available before the collision takes place can go from 1-2 days to a few hours.

According to a U.S. military analysis, an average of ten collision avoidance maneuvers were carried out every week in 2010.[1]

Collision avoidance bares an important cost for satellite operators and is very much related to the accumulation of space debris in the near future together with the improvement of ground based tracking systems. Both trends will lead to the situation in which more and more collisions with smaller and smaller fragments will be predicted. This will in the end increase the fuel and operational cost of collision avoidance and, in turn, the interest for optimum solutions. In particular, last-minute non-tangential maneuvers may become more frequent. The thrust vector direction optimization in this case is non-trivial and approximate analytical solutions would be highly desirable.

The best known analytical model describing the collision dynamics and impact probability between two orbiting objects was proposed by Akella and Alfriend in 2000.[2] Based on a uniform

*Research Fellow, Space Dynamics Group, Technical University of Madrid (UPM), Madrid, Spain

rectilinear motion approximation near the impact event they were able to accurately describe the objects relative motion and their collision probability.

Starting from a similar model, an analytical solution is here provided to describe the position shift in the collision b-plane of the two objects following a generic impulsive maneuver carried out with a given angular separation of the maneuver point with respect to the predicted collision. The model is valid for generic orbital elements of the two colliding objects and shows excellent agreement with a full numerical solutions.

Next, an optimization analysis is carried out to determine the optimum thrust direction conditions and instant of the maneuver. As expected it is seen that maneuvers carried out with an available time-span exceeding of few orbits are characterized by a nearly tangential impulse applied near to the orbit periapsis. However, last-minute maneuvers are in general counter-intuitive and strongly dependent on the encounter geometry. This is in agreement with results obtained when analyzing the optimal impulsive deflection of Earth-threatening asteroids.[3]

THE IMPULSIVE COLLISION AVOIDANCE PROBLEM

The fundamental collision avoidance problem for the case of a single impulsive maneuver can be formulated in a quite straightforward manner:

Let us suppose a collision is predicted to occur between two satellites S_1 and S_2 within a time span Δt and let the satellite S_1 be set up to perform an avoidance $\triangle$V maneuver of given magnitude along a chosen direction and time before the collision. What is the maneuver direction and instance that maximize the close-approach distance between the two objects?

In order to solve this problem while resorting to analytical expressions as much as possible the following two tasks are accomplished:

1- Provide simple approximate expressions relating the dynamical state of the two objects near the collision events to their minimum approach distance.

2- Provide simple approximate expressions relating the characteristics of the impulsive maneuver (direction and orbit location) to the dynamical state of the two objects near the collision events.

3- Solve the optimization problem to characterize the optimum $\triangle$V maneuver and its outcome.

COLLISION AVOIDANCE KINEMATICS

The kinematics of collision avoidance are analogous to the kinematics of asteroid deflection. Previous formulas[4] were derived to obtain the deflection magnitude and minimum orbit intersection distance (MOID) between a deflected asteroid and the Earth. Those formulas were restricted to the case of planar deflection maneuver and circular approximation for the Earth orbit. We here remove such approximations allowing the $\triangle$V maneuver to be applied along a direction chosen at will and by considering two generic elliptical orbits. The only simplifying assumption retained here is that the displacement of the maneuvered satellite from the impact point, as a result of the deflection action and/or any additional perturbation force, is small relatively to its radial orbital distance.

Let us employ, from now on, the radial position at collision (r) as the unit of distance and $1/n_0$ as the unit of time where n_0 is the angular rate of a *circular* orbit with radius equal to r_c:

$$n_0 = \sqrt{\frac{\mu}{r^3}},$$

with μ indicating the gravitational parameter of the Earth.

Let $< X, Y, Z >$ represent an inertial reference system with X along the unperturbed orbit eccentricity vector of the maneuverable satellite S_1, Z orthogonal to the S_1 orbit plane and Y following the right-hand rule. Let θ indicate the angle between the X axis and the position of S_1 along the orbit.

At the impact event, occurring when $\theta = \theta_c$, the non-dimensional position and velocity of the unperturbed spacecraft S_1 with respect to $< X, Y, Z >$ can be written as:

$$\mathbf{r}_1 = (r\cos\theta_c, r\sin\theta_c, 0)^{\mathrm{T}}, \tag{1}$$

$$\mathbf{v}_1 = (-q_{30}\sin\theta_c, q_{10} + q_{30}\cos\theta_c, 0)^{\mathrm{T}}, \tag{2}$$

where q_{10}, q_{30} are the generalized Pelaez' orbital elements,[56] of the initial S_1 orbit and can be related to the classical orbit eccentricity as:

$$q_{10} = \frac{e_0}{\sqrt{1 + e_0\cos\theta_c}},$$

$$q_{30} = \frac{1}{\sqrt{1 + e_0\cos\theta_c}}.$$

In addition, the radius r can be written as:

$$r = \frac{1}{q_{30}\left(q_{30} + q_{10}\cos\theta_c\right)}.$$

The velocity of S_2 at impact can be obtained by rotating the velocity of S_1 by an angle $-\pi < \phi < \pi$ around the normal to S_1 orbital plane followed by an out-of-plane rotation $-\pi/2 < \psi < \pi/2$, and by rescaling the vector magnitude by a factor χ (see Fig 1):

$$\mathrm{v}_2 = \chi \begin{pmatrix} [v_{1,1}\cos\phi - v_{1,2}\sin\phi]\cos\psi \\ [v_{1,1}\sin\phi + v_{1,2}\cos\phi]\cos\psi \\ \|\mathbf{v}_1\|\sin\psi \end{pmatrix}, \tag{3}$$

with:

$$\chi = \frac{\|\mathbf{v}_2\|}{\|\mathbf{v}_1\|}; \quad \phi = \mathrm{atan2}\left[(\mathrm{v}_1 \times \mathbf{v}_{2\perp}) \cdot \mathbf{u}_{\mathrm{h}}, \mathbf{v}_1 \cdot \mathbf{v}_{2\perp}\right]; \quad \psi = \mathrm{atan2}\left[(\mathbf{v}_{2\perp} \times \mathbf{v}_2) \cdot \mathbf{u}_{\mathrm{d}}, \mathbf{v}_2 \cdot \mathbf{v}_{2\perp}\right];$$

where:

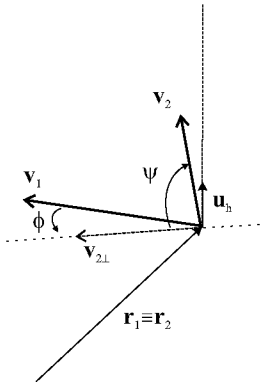

Figure 1. geometrical relation between v_1 and $\mathbf{v}_2$ at collision.

$$\mathbf{u}_\mathrm{h} = \frac{\mathbf{r}_1 \times \mathbf{v}_1}{\|\mathbf{r}_1 \times \mathbf{v}_1\|}; \quad \mathbf{v}_{2\perp} = \mathbf{v}_2 - (\mathbf{v}_2 \cdot \mathbf{u}_\mathrm{h})\,\mathbf{u}_\mathrm{h}; \qquad \mathbf{u}_\mathrm{d} = \frac{\mathrm{v}_{2\perp} \times \mathbf{u}_\mathrm{h}}{\|\mathbf{v}_{2\perp} \times \mathbf{u}_\mathrm{h}\|};$$

By excluding the unlikely case in which v_1 and $\mathbf{v}_2$ are parallel let $< x, y, z >$ represent an inertial reference system centered at the $S_1 - S_2$ impact point and with axes directions defined as:

$$\mathbf{u}_x = \frac{\boldsymbol{v}_1}{\|\boldsymbol{v}_1\|}, \quad \mathbf{u}_z = \frac{\boldsymbol{v}_1 \times \boldsymbol{v}_2}{\|\boldsymbol{v}_1 \times \boldsymbol{v}_2\|}, \quad \mathbf{u}_y = \mathbf{u}_z \times \mathbf{u}_x.$$

Within a small interval of time $\Delta t \ll 1$ around the impact event, we can consider the motion of both objects as *uniform rectilinear* with good approximation. In this hypothesis the trajectories of the two bodies are represented by two straight lines in the unperturbed $< x, y >$ plane and intersecting with each other at the time of the impact.

If one assumes a deflection maneuver is applied to S_1, its velocity vector at the impact event can be considered virtually unchanged with respect to the unperturbed case [*]. Conversely, S_1 position at the impact event will have shifted from the origin of $< x, y, z >$ to the point $(\delta x, \delta y, \delta z)^\mathrm{T}$. Under the uniform rectilinear motion assumption, the corresponding shift of S_1 image in the b-plane of S_2 can be determined with simple geometrical considerations as done in the following.

First of all, the $< \xi, \eta, \zeta >$ b-plane frame centered at S_2 is considered.[7] This frame is characterized by having the η axis directed along S_1 velocity relative to S_2, the ζ axis in the direction opposite to the projection on the b-plane of the velocity of S_2 and ξ following the right-hand rule. The ξ axis, which as shown in the previous reference corresponds to the direction of the minimum orbit intersection distance (MOID), is orthogonal to the geocentric velocity vectors $\boldsymbol{v}_1$ and $\boldsymbol{v}_2$, and coincides with the previously defined z axis.

With reference to Fig. (2) the image on the b-plane of a point $(\delta x, \delta y, \delta z)^\mathrm{T}$ obeys:

$$\begin{cases} \xi = -\delta z \\ \zeta = -\delta x \, \sin\beta - \delta y \, \cos\beta \end{cases}, \tag{4}$$

[*]Typical collision avoidance maneuvers involve velocity changes of the order of m/s, completely negligible when compared to their orbital velocity

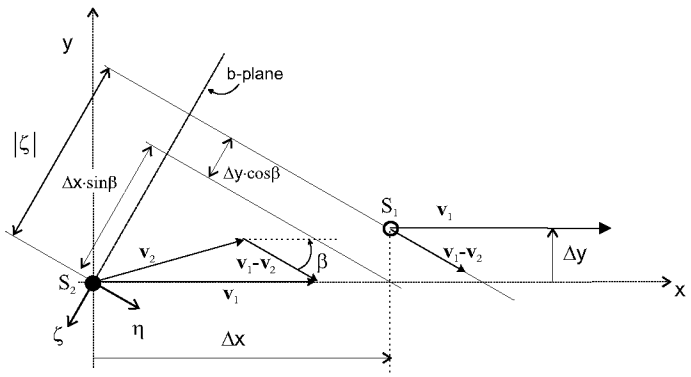

Figure 2. Snapshot of $S_1 - S_2$ encounter geometry (x-y plane) after the ACA maneuver

where $0 < \beta \leq \pi$ is the angle between the inertial velocity of S_1 and the velocity of S_1 relative to S_2.

The total collision miss distance results in:

$$\rho = \sqrt{\xi^2 + \zeta^2}. \tag{5}$$

One now needs to relate δx , δy and δz to the characteristics of the perturbed orbital motion of S_1.

When S_1 reaches the impact angular position θ_c it will have accumulated, in the most general case, an orbital radius variation δr, a time delay δt when compared to its original unperturbed trajectory and an out of plane displacement δw. Because of the uniform rectilinear motion approximation, the accumulated time delay δt gives rise to a position shift along the velocity vector and its contribution can be written as:

$$\delta x' = -v_1 \delta t, \tag{6}$$

where v_1 can be taken as the magnitude of the unperturbed velocity $\mathbf{v}_1$ at impact, which can be computed directly from Eq.(2) as:

$$v_1 = \sqrt{q_{10}^2 + 2q_{10}q_{30}\cos\theta_c + q_{30}^2}. \tag{7}$$

On the other hand, the variations δr and δw affect in general all three components of the position shift as:

$$\delta x'' = \delta r(\mathbf{u}_r \cdot \mathbf{u}_x) + \delta w(\mathbf{u}_w \cdot \mathrm{u}_x), \tag{8}$$

$$\delta y = \delta r(\mathrm{u}_r \cdot \mathbf{u}_y) + \delta w(\mathbf{u}_w \cdot \mathrm{u}_y), \tag{9}$$

$$\delta z = \delta r(\mathbf{u}_r \cdot \mathbf{u}_z) + \delta w(\mathbf{u}_w \cdot \mathbf{u}_z), \tag{10}$$

where:

$$\mathbf{u}_r = (\cos\theta_c, \sin\theta_c, 0)^T, \tag{11}$$

$$\mathbf{u}_w = (0, 0, 1)^T, \tag{12}$$

By employing Eqs. (2,3) and after some algebraic simplifications Eq. (8) yields:

$$\delta x'' = \frac{q_{10}\sin\theta_c}{v_1}\delta r.$$

The overall displacement along x is then:

$$\delta x = \delta x' + \delta x''. \tag{13}$$

Similarly, Eqs. (9,10) can be put in the form:

$$\delta y = -\frac{(q_{30} + \cos\theta_c q_{10})\cos\psi\sin\phi}{v_1\sqrt{1-\cos^2\psi\cos^2\phi}}\delta r + \frac{\sin\psi}{\sqrt{1-\cos^2\psi\cos^2\phi}}\delta w, \tag{14}$$

$$\delta z = \frac{(q_{30} + \cos\theta_0 q_{10})\sin\psi}{v_1\sqrt{1-\cos^2\psi\cos^2\phi}}\delta r + \frac{\cos\psi\sin\phi}{\sqrt{1-\cos^2\psi\cos^2\phi}}\delta w. \tag{15}$$

Grouping the three previous equations together one obtains:

$$\begin{pmatrix} \delta x \\ \\ \delta y \\ \\ \delta z \end{pmatrix} = \begin{pmatrix} -v_1 & \sin\alpha\sin\theta_c & 0 \\ \\ 0 & -\dfrac{\cos\alpha\sin\phi\cos\psi}{\sqrt{1-\cos^2\psi\cos^2\phi}} & \dfrac{\sin\psi}{\sqrt{1-\cos^2\psi\cos^2\phi}} \\ \\ 0 & \dfrac{\cos\alpha\sin\psi}{\sqrt{1-\cos^2\psi\cos^2\phi}} & \dfrac{\sin\phi\cos\psi}{\sqrt{1-\cos^2\psi\cos^2\phi}} \end{pmatrix} \begin{pmatrix} \delta t \\ \\ \delta r \\ \\ \delta w \end{pmatrix}, \tag{16}$$

where α is the *flight path angle* at collision, which obeys:

$$\sin\alpha = \frac{q_{10}\sin\theta_c}{v_1}; \qquad \cos\alpha = \frac{q_{30} + q_{10}\cos\theta_c}{v_1}.$$

Finally the angle β can be expressed as:

$$\cos\beta = \frac{(\mathbf{v}_1 - \mathbf{v}_2)\cdot\mathbf{v}_1}{\|\mathbf{v}_1\|\,\|\mathrm{v}_1 - \mathbf{v}_2\|} = \frac{1 - \chi\cos\psi\cos\phi}{\sqrt{1 - 2\chi\cos\psi\cos\phi + \chi^2}}, \tag{17}$$

$$\sin\beta = \sqrt{1-\cos^2\beta}. \tag{18}$$

What is left to compute is the accumulated delay δt, radial and out of plane variation δr and δw for S_1 along the orbit arc $\theta_m - \theta_c$ following a given impulsive avoidance maneuver.

COLLISION AVOIDANCE DYNAMICS

Generalized orbital elements variation

Let us assume a collision avoidance impulsive maneuver is carried out at the orbital position (r_m, θ_m) with radial, transverse and out-of-plane impulsive velocity variations ΔV_r, ΔV_θ, and ΔV_h, respectively.

The non-dimensional velocity variations:

$$(\triangle v_r, \triangle v_\theta, \triangle v_h) = (\triangle V_r, \triangle V_\theta, \triangle V_h) / \sqrt{\frac{\mu}{r_c}},$$

are all small quantities, as long as the total maneuver ΔV is small compared to S_1 orbital velocity. One can then express the resulting post-maneuver generalized orbital elements as:

$$q_1 \sim q_{10} + Q_{1\theta} \triangle v_\theta + Q_{1r} \triangle v_r \tag{19}$$

$$q_2 \sim Q_{2\theta} \triangle v_\theta + Q_{2r} \triangle v_r \tag{20}$$

$$q_3 \sim q_{30} + Q_{3\theta} \triangle v_\theta \tag{21}$$

The functions Q_i can be obtained following from the variational equations of the transverse and radial orbital velocity:

$$s = s_0 + \triangle v_\theta = q_{30} + q_{10} \cos\theta_m + \triangle v_\theta$$

$$u = u_0 + \triangle v_r = q_{10} \sin\theta_m + \triangle v_r$$

and from the relations:

$$q_3 = \frac{1}{r_m s} \tag{22}$$

$$q_1 = (s - q_3) \cos\theta_m + u \sin\theta_m \tag{23}$$

$$q_2 = (s - q_3) \sin\theta_m - u \cos\theta_m \tag{24}$$

with:

$$r_m = \frac{1}{q_{30} \left(q_{30} + q_{10} \cos\theta_m\right)}.$$

By substituting Eqs. (22-24) into Eqs. (19-21), expanding in Taylor series for small $(\triangle v_r, \triangle v_\theta)$ and solving for Q_i one finally obtains:

$$Q_{1\theta}(\theta_m) = \frac{(2q_{30} + q_{10}\cos\theta_m)\cos\theta_m}{q_{30} + q_{10}\cos\theta_m},$$

$$Q_{1r}(\theta_m) = \sin\theta_m,$$

$$Q_{2\theta}(\theta_m) = \frac{(2q_{30} + q_{10}\cos\theta_m)\sin\theta_m}{q_{30} + q_{10}\cos\theta_m},$$

$$Q_{2r}(\theta_m) = -\cos\theta_m,$$

$$Q_{3\theta}(\theta_m) = -\frac{q_{30}}{q_{30} + q_{10}\cos\theta_m}.$$

In-plane dynamics: radial shift

The orbit radius variation of S_1 at $\theta = \theta_c$ following the collision avoidance maneuver obeys:

$$\delta r = \frac{1}{q_{30}(q_{30} + q_{10}\cos\theta_c)} - \frac{1}{q_3(q_3 + q_1\cos\theta_c + q_2\sin\theta_c)}.$$

By substituting the first-order expressions of q_i derived above one obtains:

$$\delta r \approx C_{r\theta}\triangle v_\theta + C_{rr}\triangle v_r,$$

where the functions C_i read:

$$C_{r\theta} = \frac{2q_{30}[1 - \cos(\theta_c - \theta_m)] - q_{10}\sin(\theta_m)\sin(\theta_c - \theta_m)}{q_{30}(q_{30} + q_{10}\cos\theta_m)(q_{30} + q_{10}\cos\theta_c)^2},$$

$$C_{rr} = \frac{\sin(\theta_c - \theta_m)}{q30(q_{30} + q_{10}\cos\theta_c)^2}$$

In-plane dynamics: phasing

The time elapsed along the arc $[\theta_m;\ \theta_c]$ can be obtained by integrating the Sundman transformation:

$$\triangle t = \int_{\theta_m}^{\theta_c} \frac{d\theta}{q_3 s^2}. \tag{25}$$

where:

$$s = q_3 + q_1\cos\theta + q_2\sin\theta.$$

Eq (25) can be integrated and written in the form:

$$\Delta t = \Delta t_0 + \delta t,$$

where Δt_0 is the elapsed time along the initial Keplerian orbit and δt is the time delay caused by the impulsive ΔV maneuver.

The termΔt_0 follows Kepler´s equation and can be written in terms of the Pelaez' element set as:

$$\Delta t_0 = \frac{q_{30}\left(E_c - E_m\right) - q_{10}\left(\sin E_c - \sin E_m\right)}{\left(q_{30}^2 - q_{10}^2\right)^{3/2}},$$

with E_m,E_c corresponding to the eccentric anomalies at the maneuver and collision location of the initial S_1 orbit.

After making use of the expressions (19-21) and expanding in Taylor series for small $(\triangle v_\theta, \triangle v_r)$ the time delay δt follows:

$$\delta t = C_{t\theta} \triangle v_\theta + C_{tr} \triangle v_r,$$

with:

$$\begin{aligned} C_{t\theta} \;=\; & \frac{1}{q_{30}\left(q_{30}^2 - q_{10}^2\right)^{5/2}\left(q_{30} - q_{10}\cos E_m\right)} \times \left[K_{\theta 1}\left(E_c - E_m\right) + \right. \\ & + K_{\theta 2}\left(\sin E_c - \sin E_m\right) + K_{\theta 3}\left(\sin 2E_c - \sin 2E_m\right) + \\ & \left. + K_{\theta 4}\left(\cos E_c - \cos E_m\right) + K_{\theta 5}\left(\cos 2E_c - \cos 2E_m\right)\right] \end{aligned}$$

where:

$$K_{\theta 1} = 3q_{30}\left(q_{30}^2 - q_{10}^2\right)$$

$$K_{\theta 2} = \frac{1}{2}\left[3q_{10}^3 - \left(2q_{30}^2 - q_{10}^2\right)\left(4q_{30}\cos E_m - q_{10}\cos 2E_m\right)\right]$$

$$K_{\theta 3} = \frac{q_{10}\, q_{30}}{4}\left[4q_{30}\cos E_m - q_{10}\left(3 + \cos 2E_m\right)\right]$$

$$K_{\theta 4} = q_{30}\left[\left(4{q_{30}}^2 - 2q_{10}^2\right)\sin E_m - q_{10}\, q_{30}\sin 2E_m\right]$$

$$K_{\theta 5} = -\frac{q_{10}}{4}\left[\left(4{q_{30}}^2 - 2q_{10}^2\right)\sin E_m - q_{10}\, q_{30}\sin 2E_m\right]$$

and:

$$
\begin{aligned}
C_{tr} &= \frac{1}{q_{30}\left(q_{30}^2 - q_{10}^2\right)^2 \left(q_{30} - q_{10}\cos E_m\right)} \times \left[K_{r1}\left(E_c - E_m\right) + \right. \\
&+ K_{r2}\left(\sin E_c - \sin E_m\right) + K_{r3}\left(\sin 2E_c - \sin 2E_m\right) + \\
&\left. + K_{r4}\left(\cos E_c - \cos E_m\right) + K_{r5}\left(\cos 2E_c - \cos 2E_m\right)\right]
\end{aligned}
$$

$$
K_{r1} = 3 q_{10} q_{30} \sin E_m
$$

$$
K_{r2} = -2\left({q_{30}}^2 + {q_{10}}^2\right) \sin E_m
$$

$$
K_{r3} = \frac{q_{10} q_{30}}{2} \sin E_m
$$

$$
K_{r4} = -2 q_{30}\left(q_{30}\cos E_m - q_{10}\right)
$$

$$
K_{r5} = \frac{q_{10}}{2}\left(q_{30}\cos E_m - q_{10}\right).
$$

Out-of-plane dynamics: phasing

The out of plane motion is decoupled from the planar one and can be described with sufficient accuracy by linearizing the gravitational acceleration (Lawden's Equations).

A closed form analytical solution of the out-of-plane Lawden's equation can be found by using the true anomaly as independent variable as done by Yamanaka-Ankersen.[8] From that reference, and indicating with p_0 the initial orbital parameter, the dimensional out-of-plane displacement can be written as:

$$
\Delta Z = \sqrt{\frac{p_0^3}{\mu}} \frac{\sin\left(\theta_c - \theta_m\right)}{\left(1 + e_0\cos\theta_m\right)\left(1 + e_0\cos\theta_c\right)} \Delta V_h,
$$

and after re-scaling the different quantities according to the present non-dimensionalization one obtains:

$$
\Delta w = \frac{\sqrt{q_{30}^2 + q_{10} q_{30}\cos\theta_c}}{q_{30} + q_{10}\cos\theta_m} \sin\left(\theta_c - \theta_m\right) \Delta v_h
$$

MANEUVER OPTIMIZATION

In this section three numerical examples of collision avoidance will be considered, the first based on the 2009 Iridium-Cosmos collision, the second based on a highly elliptical orbit (e=0.99) for the maneuverable satellite and the third involving a near head-on collision. The examples will be employed to study the optimum maneuver direction and orbit location in order to maximize the collision miss distance. A test of the accuracy of the proposed analytical formulation will also be conducted.

The radial, transverse and out-of-plane component of the maneuver velocity vector can be conveniently expressed as:

$$\triangle V_r = \triangle V \cos\gamma \sin(\sigma + \alpha)$$

$$\triangle V_\theta = \triangle V \cos\gamma \cos(\sigma + \alpha)$$

$$\triangle V_h = \triangle V \sin\gamma$$

where α is the flight path angle, σ is the in-plane rotation, opposite to the orbit angular momentum, of the maneuver velocity vector with respect to *tangent to the orbit*, and γ is the subsequent rotation along the out-of-plane direction.

Iridium-Cosmos collision

The 2009 Iridium-Cosmos collision took place on February 10 2009 and saw the active Iridium 33 spacecraft impacting the disabled Cosmos 2251 satellite at roughly 788.6 km altitude above Siberia. After considering Iridium 33 as the maneuverable spacecraft (S_1) and processing the two-line elements data available from Space-Track one can derive all the necessary parameters (see table 1) to evaluate the outcome of a possible collision avoidance maneuver. The maximum achievable deflection is plotted in Fig 3 and can be obtained with the optimal control ΔV orientation plotted in Fig 4. The results confirm the known fact that the optimal maneuver orientation is nearly tangential when applied more than one orbit before the impact and far from tangential when applied during the last orbit (see for instance[3]). The difference in achievable miss distance when comparing a tangential and optimal maneuver is in any case relatively small (Fig. 5).

A comparison between the present analytical formulation and a full numerical analysis shows a negligible error (less than 0.1% in this case) (see Fig. 6).

Table 1. Iridium-Cosmos encounter geometry. Here Iridium is the maneuverable satellite (S_1).

a_0(km)	e_0	ϕ(deg)	ψ(deg)	θ_c(deg)	χ
7155.8	2×10^{-4}	180.0	77.5	-16.85	1.0

Highly eccentric orbit

A collision avoidance based on a highly eccentric orbit (e=0.95) for the maneuverable spacecraft is now considered, whose characteristics are listed in table 2. The maximum achievable deflection

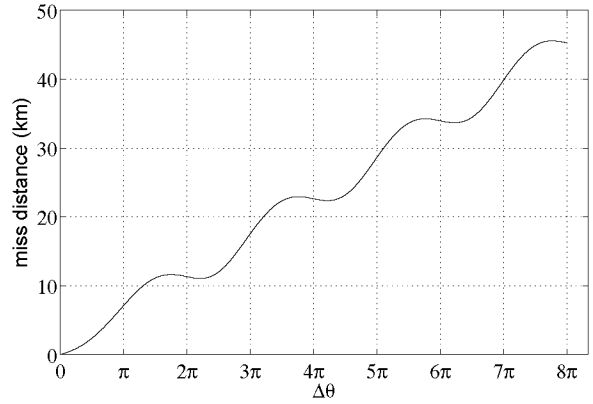

Figure 3. Maximum achievable miss distance (km) as a function of the maneuver separation arc for the Iridium-Cosmos collision (Table 1). A ΔV maneuver of 1 m/s is assumed.

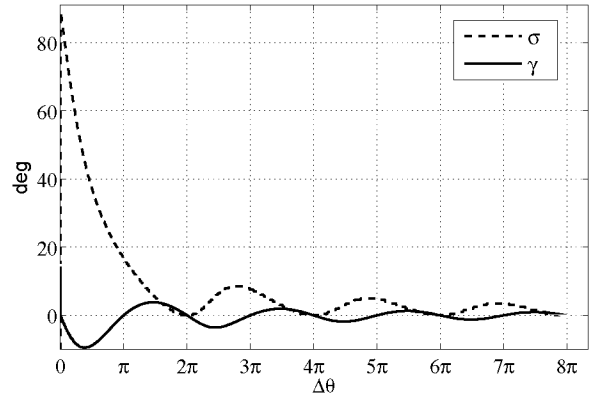

Figure 4. Optimal maneuver direction angles relative to Fig 3.

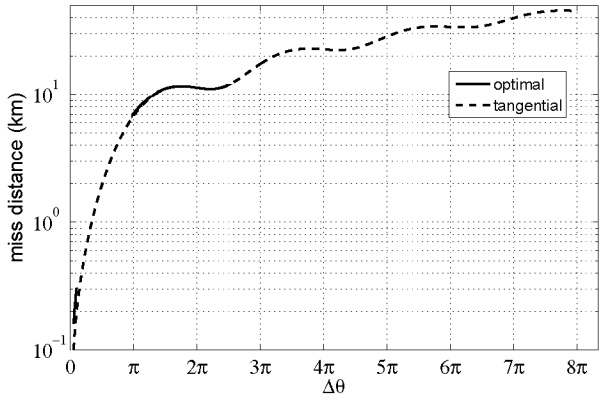

Figure 5. Miss distance (see Fig 3) obtained with optimal and tangential maneuver direction.

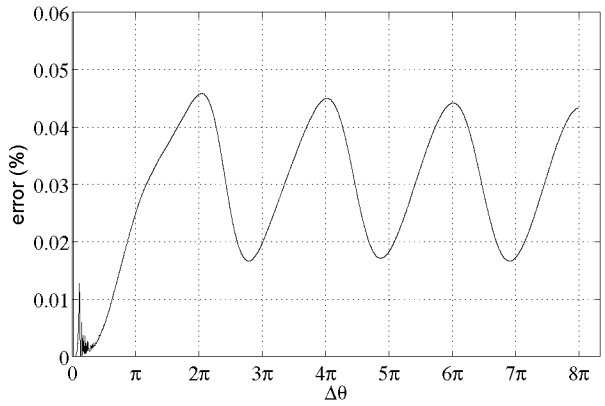

Figure 6. Relative error (%) of the present analytical formulation for the computation of the miss distance (Fig 3). A high-accuracy numerical integration is employed for the comparison.

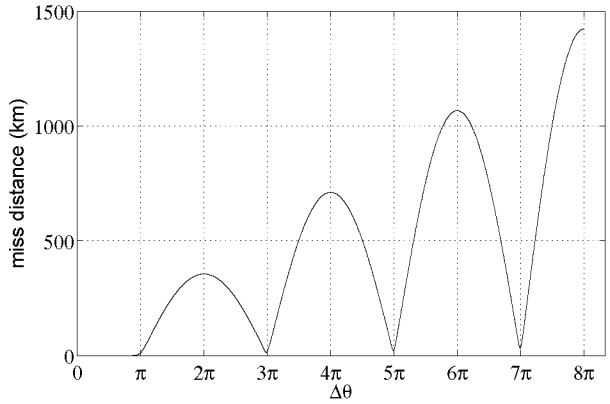

Figure 7. Maximum achievable miss distance (km) as a function of the maneuver separation arc for the high-eccentricity collision (Table 2). A ΔV maneuver of 1 cm/s is assumed.

plot of Fig. (7) highlights the importance of performing the maneuver near periapsis, as it is well known. Also, and similarly to the Iridium-Cosmos example, the optimal maneuver orientation is nearly tangential when applied more than one orbit before the impact and far from tangential when applied during the last orbit (Fig. (8)). The difference in achievable miss distance when comparing a tangential and optimal maneuver is again relatively small but more significant for a maneuver performed during the last orbit (Fig. 9).

A comparison between the present analytical formulation and a full numerical analysis shows a negligible error (less than 1% in this case) (see Fig. 10).

Table 2. Highly eccentric orbit encounter geometry.

a_0(km)	e_0	ϕ(deg)	ψ(deg)	θ_c(deg)	χ
133560.0 km	0.95	180.0	77.5	0	1.0

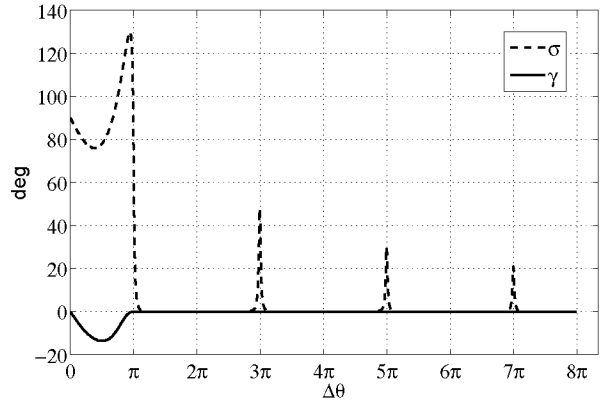

Figure 8. Optimal maneuver direction angles relative to Fig 7.

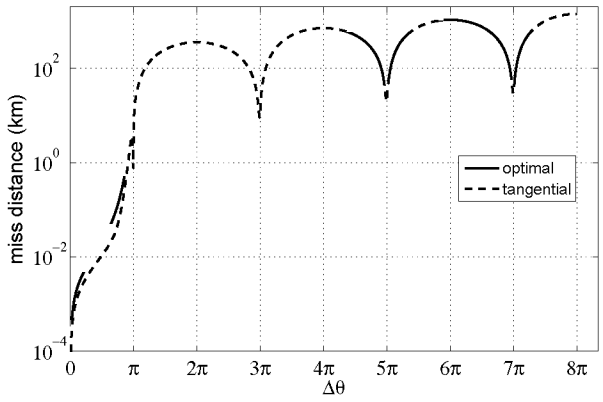

Figure 9. Miss distance (see Fig 7) obtained with optimal and tangential maneuver direction.

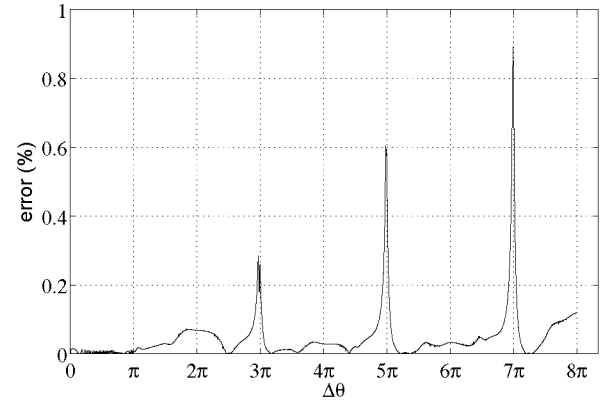

Figure 10. Relative error (%) of the present analytical formulation for the computation of the miss distance (Fig 7). A high-accuracy numerical integration is employed for the comparison.

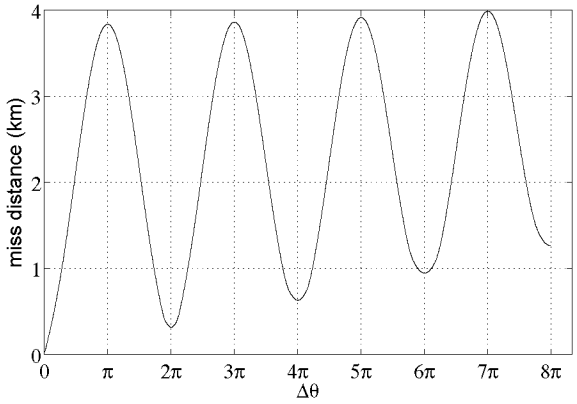

Figure 11. Maximum achievable miss distance (km) as a function of the maneuver separation arc for the high-eccentricity collision (Table 2). A ΔV maneuver of 1 cm/s is assumed.

Near head-on collision

The last example is based on a near head-on collision between two nearly circular orbits. This particular example is very relevant to the current LEO environment characterized by two large sun-synchronous spacecraft populations around 98 and 82 degrees inclination. When such condition occurs the phasing term and its secular increase can no longer be exploited and the total deflection is dominated by the (non-secular) orbit radius variation, which are maximized when the maneuver is executed (n+1/2) orbits before the impact. Fig. (11) highlights this aspect and the higher cost of a collision avoidance maneuver when applied to near head-on collisions. The optimum maneuver orientation (Fig. (12)) shows an interesting structure although under optimal maneuver phasing the velocity variation vector is practically tangent to the orbit (see also Fig. (13)). Finally, even in this case the proposed analytical formulation exhibits negligible error as seen in Fig (14).

Table 3. Near head-on collision

a_0(km)	e_0	ϕ(deg)	ψ(deg)	θ_c(deg)	χ
7155.8	2×10^{-4}	180.0	2.0	-16.85	1.0

CONCLUSIONS

The problem of optimal impulsive collision avoidance between two spacecraft in generic Keplerian orbits has been investigated. Very accurate and relatively simple analytical expressions have been provided to compute the impact miss distance given the characteristics of the orbit of the maneuverable spacecraft, the encounter geometry and the maneuver characterization (magnitude, orientation and phasing). The expressions show negligible errors even for extreme conditions (very high eccentricity orbits). Based on these expressions a full three-dimensional optimization of the delta-V impulse direction has been conducted. Tangential maneuvers are seen to be near optimal when sufficient warning time is available (more than 1 orbit) but the optimum maneuver phasing is highly dependent on the type of orbit and conjunction geometry.

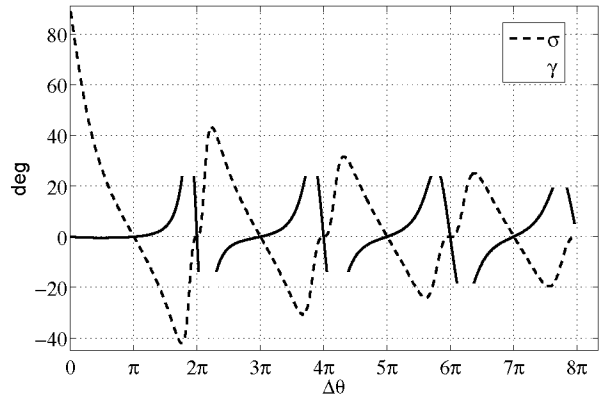

Figure 12. Optimal maneuver direction angles relative to Fig 11.

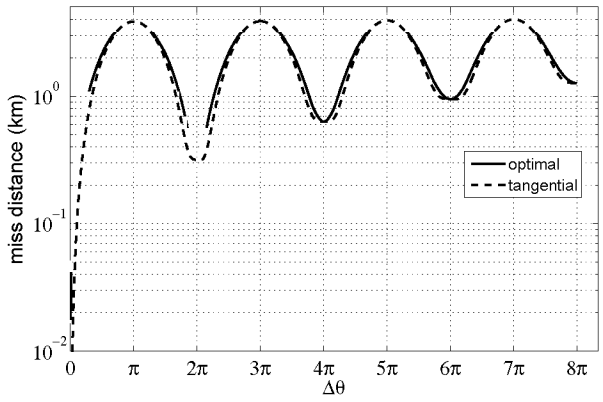

Figure 13. Miss distance (see Fig 11) obtained with optimal and tangential maneuver direction.

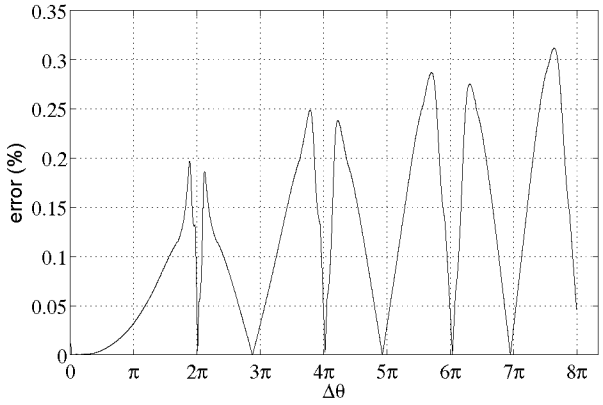

Figure 14. Relative error (%) of the present analytical formulation for the computation of the miss distance (Fig 11). A high-accuracy numerical integration is employed for the comparison.

ACKNOWLEDGMENTS

The study has been supported by the research project "Dynamic Simulation of Complex Space Systems" supported by the Dirección General de Investigación of the (former) Spanish Ministry of Science and Innovation through contract AYA2010- 18796.

REFERENCES

[1] "Towards Long-term Sustainability of Space Activities: Overcoming the Challenge of Space Debris," tech. rep., 03-02-2011. Available on line at http://www.oosa.unvienna.org.

[2] M. Akella and K. Alfriend, "Probability of Collision Between Space Objects," *Journal of Guidance, Control and Dynamics*, Vol. 23, No. 5, 2000, pp. 769–772.

[3] R. Kahle, G. Hahn, and E. Kuhrt, "Optimal deflection of NEOs en route of collision with the Earth," *Icarus*, Vol. 182, No. 2, 2006, pp. 482–488.

[4] C. Bombardelli and G. Baù, "Accurate analytical approximation of asteroid deflection with constant tangential thrust," *Celestial Mechanics and Dynamical Astronomy*, 2012, pp. 1–17.

[5] J. Pelaez, J. Hedo, and P. d. Andres, "A special perturbation method in orbital dynamics," *Celestial Mechanics and Dynamical Astronomy*, Vol. 97, No. 2, 2007, pp. 131–150.

[6] C. Bombardelli, G. Bau, and J. Pelaez, "Asymptotic Solution for the Two-Body Problem with Constant Tangential Thrust Acceleration," *Celestial Mechanics and Dynamical Astronomy*, Vol. 110, No. 3, 2011, pp. 239–256.

[7] G. Valsecchi, A. Milani, G. Gronchi, and S. Chesley, "Resonant returns to close approaches: Analytical theory," *Astronomy and Astrophysics*, Vol. 408, No. 3, 2003, pp. 1179–1196.

[8] K. Yamanaka and F. Ankersen, "New State Transition Matrix for Relative Motion on an Arbitrary Elliptical Orbit," *Journal of guidance, control and dynamics*, Vol. 25, No. 1, 2002, pp. 60–66.